ENGINEERING PROGRESS
at the
University of Florida

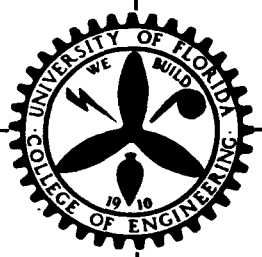

Vol. XVII, No. 6

June, 1963

TECHNICAL PAPER NO. 263

Elastic Instability of Pressurized Cylindrical Shells Under Compression or Bending

by

S. Y. Lu and W. A. Nash

Advanced Engineering Mechanics Section
University of Florida

Reprinted from *Proceedings of the Fourth U. S. National Congress of Applied Mechanics*, Vol. 1, held at the University of California June 18-21, 1962.

Published monthly by the

FLORIDA ENGINEERING AND INDUSTRIAL EXPERIMENT STATION

COLLEGE OF ENGINEERING UNIVERSITY OF FLORIDA GAINESVILLE

Entered as second-class matter at the Post Office at Gainesville, Florida

The elastic stability of circular cylindrical shells subject to either axial compression or pure bending is investigated for the case of cylinders strengthened by internal pressure. Nonlinear finite deflection theory is employed and an approximate solution of the equilibrium and compatibility equations is obtained by use of Galerkin's method. Comparatively simple expressions are presented for the various buckling stresses and these expressions are evaluated to yield buckling stresses as a function of the internal pressure. The critical stress for bending is found to be greater than that in axial compression, and in approximately the ratio indicated by recent experimental evidence.

Elastic instability of pressurized cylindrical shells under compression or bending.

S. Y. Lu
W. A. Nash
University of Florida

Nomenclature

D	Flexural rigidity $Et^3/12(1-\nu^2)$
E	Young's modulus
F	Airy stress function
R	Radius of middle surface of shell
m, n	Number of waves in axial and circumferential directions respectively
p	Internal pressure
t	Wall thickness of shell
w	Radial deflection
x, s	Co-ordinates of a point in the middle surface of the shell, measured in the longitudinal and circumferential directions respectively.
α	R/tm^2
η	$b_3/t\alpha$
μ	n^2/m^2
ν	Poisson's ratio, $\nu = 0.3$ in present study
ϕ, ϕ_b	Dimensionless stress parameters
$\sigma, \sigma_b, \sigma_c$	Axial compressive stresses
∇^2	Laplace operator
∇^4	$(\nabla^2)^2$

Subscripts:

b	Bending
cr	Critical condition
o	No Pressure

[1] The present investigation was sponsored by the National Aeronautics and Space Administration under Research Grant NsG-16-59.

Introduction

The postbuckling behavior of cylindrical shells subject to axial compression has been studied by several investigators. Donnell [1] first derived the governing finite-deflection equations; later, in 1941, these equations were used by von Kármán and Tsien [2] to obtain an approximate solution to the problem of buckling of an axially compressed cylinder into a diamond shaped buckle pattern. Further investigation was made by Kempner [3] who used an additional parameter in the buckling deflection function proposed in [2]. Several variations of these analyses have been proposed by other investigators.

The increase in stability of internally pressurized cylindrical shells subject to axisymmetric loading was studied by Lo, Crate, and Schwartz [4]. They used large-deflection theory and found that the critical stress increases from a value of 0.37 Et/R at zero pressure to 0.606 Et/R (i.e., the value given by classical small deflection theory) as the pressure increases to $0.2\,Et^2/R^2$. Very recently, the effect of internal pressurization on stability of axially compressed cylinders was studied by Thielemann [5]. In addition to presenting a finite deflection theory, he also conducted tests on aluminum shells. All the aforementioned analytical solutions were obtained on the basis of the energy criterion.

Seide [8] has recently presented a linear small deflection analysis of the buckling of cylindrical shells subject to pure bending. This study indicated that, contrary to the commonly accepted value, the maximum critical

bending stress is for all practical purposes equal to the critical stress found for axial compression. This result, based upon small deflection theory, does not offer any explanation of the experimental differences known to exist for these two situations. For example, experimental evidence due to Suer, Harris, Skene, and Benjamin [9] indicates buckling loads in bending to be from 25 to 60 per cent greater than in compression, the exact value depending upon the ratio R/t.

This report is a study of the elastic postbuckling behavior of thin pressurized cylinders subject to bending loads. Throughout this analysis, the Galerkin method is employed. For comparison with certain existing results obtained by using the energy method, a solution for shells subject to axisymmetric compression is reached first. For this case, when the pressure parameter pR^2/Et^2 approaches unity, it is found that the solution is the same as the classical small-deflection solution.

The relation of the critical stress to internal pressure has been found. For this purpose it is convenient to introduce as a parameter the ratio between the increment of critical stress and the critical stress at zero pressure. This parameter will be essentially independent of the imperfections in the shell when the imperfections do not vary significantly due to changes in pressure. Finally, experimental data due to Suer, Harris, Skene, and Benjamin [9] are compared with the results of the present analysis.

Basic Equations and Deflection Function

For an initially perfect thin cylindrical shell the compatibility and equilibrium equations can be expressed, respectively, as

$$\nabla^4 F - E\left[\left(\frac{\partial^2 w}{\partial x \partial s}\right)^2 - \frac{\partial^2 w}{\partial x^2}\frac{\partial^2 w}{\partial s^2} - \frac{1}{R}\frac{\partial^2 w}{\partial x^2}\right] = 0 \tag{1}$$

$$D\nabla^4 w - \frac{t}{R}\frac{\partial^2 F}{\partial x^2} - t\left[\frac{\partial^2 F}{\partial s^2}\frac{\partial^2 w}{\partial x^2} - 2\frac{\partial^2 F}{\partial x \partial s}\frac{\partial^2 w}{\partial x \partial s} + \frac{\partial^2 F}{\partial x^2}\frac{\partial^2 w}{\partial s^2}\right] + p = 0 \tag{2}$$

In the above equations, F is the Airy stress function of the membrane stresses, w is the radial deflection, t the shell thickness, R the radius of the middle surface, and p is internal pressure (taken to be positive).

An approximate form of the deflection pattern is assumed:

$$w = b_1 + \cos^{\gamma}\left(\frac{ks}{2R}\right)\left[b_2 \cos\frac{mx}{R}\cos\frac{ns}{R} + b_3 \cos\frac{2mx}{R} + b_3 \cos\frac{2ns}{R}\right] \tag{3}$$

where $k = \begin{cases} 0 \text{ for a shell subject to axial compression} \\ 1 \text{ for a shell subject to eccentric compression or pure bending} \end{cases}$

$\gamma =$ even integer

and m and n represent the number of waves in the axial and circumferential directions respectively, the number of waves in the axial direction being within a length equal to the circumference of the cylinder. Throughout the present study, $\gamma = 2$. For more localized buckling, a larger value of γ could be used. When $k = 0$, (3) is the same as that used in [2]. In (3), b is not an independent parameter but is used to satisfy the condition of periodicity of circumferential displacement [3]. Corresponding to (3), an expression for the stress function F is proposed

$$F = -\frac{\sigma_c}{2}s^2 + \sigma_b R^2 \cos\frac{s}{R} + \frac{1}{2}\frac{pR}{t}x^2 + a_{11}\cos\frac{mx}{R}\cos\frac{ns}{R} + a_{22}\cos\frac{2mx}{R}\cos\frac{2ns}{R} + a_{20}\cos\frac{2mx}{R} + a_{02}\cos\frac{2ns}{R} \tag{4}$$

The stresses σ_c and σ_b are due to axial compression and bending, respectively, and are positive for compression. For shells subject to axisymmetric compression only, $\sigma_b = 0$ and σ_c is replaced by σ to avoid any possible confusion in notation.

Method of Solution

When w and F in (3) and (4) are substituted in (1) and (2), the equalities generally will not hold. They can, however, be expressed instead as

$$\nabla^4 F - E\left[\left(\frac{\partial^2 w}{\partial x \partial s}\right)^2 - \frac{\partial^2 w}{\partial x^2}\frac{\partial^2 w}{\partial s^2} - \frac{1}{R}\frac{\partial^2 w}{\partial x^2}\right] = Q_1 \tag{5}$$

and

$$D\nabla^2 w - \frac{t}{R}\frac{\partial^2 F}{\partial x^2} - t\left[\frac{\partial^2 F}{\partial s^2}\frac{\partial^2 w}{\partial x^2} - 2\frac{\partial^2 F}{\partial x \partial s}\frac{\partial^2 w}{\partial x \partial s} + \frac{\partial^2 F}{\partial x^2}\frac{\partial^2 w}{\partial s^2}\right] + p = Q_2 \tag{6}$$

An approximate solution is obtained by minimizing Q_1 and Q_2 on the right-hand sides of the above equations; this is done by the Galerkin method.

The Galerkin method establishes the following set of equations:

$$\left.\begin{aligned} &\int_0^L \int_0^{2\pi R} Q_1 \cos\frac{mx}{R}\cos\frac{ns}{R}\,ds\,dx = 0 \\ &\int_0^L \int_0^{2\pi R} Q_1 \cos\frac{2mx}{R}\cos\frac{2ns}{R}\,ds\,dx = 0 \\ &\int_0^L \int_0^{2\pi R} Q_1 \cos\frac{2mx}{R}\,ds\,dx = 0 \\ &\int_0^L \int_0^{2\pi R} Q_1 \cos\frac{2ns}{R}\,ds\,dx = 0 \end{aligned}\right\} \tag{7}$$

$$\left.\begin{aligned}\int_0^L \int_0^{2\pi R} Q_2 \cos\frac{mx}{R}\cos\frac{ns}{R}\cos^2\left(\frac{ks}{2R}\right)ds\,dx = 0\\ \int_0^L \int_0^{2\pi R} Q_2 \left(\cos\frac{2mx}{R}+\cos\frac{2ns}{R}\right)\cos^2\left(\frac{ks}{2R}\right)ds\,dx = 0\end{aligned}\right\} \quad (8)$$

Again, $k = 0$ when the shell is subject to axial compression only. In the following sections, solutions are obtained for axial compression and bending separately, although the approaches are the same.

Axisymmetric Compression

In this section, the parameter k in (3) and (8) and also σ_b in (4) are zero. Also, σ_c in (4) is replaced by σ. The coefficients a_{20}, a_{02}, a_{11}, and a_{22} appearing in (4) can be expressed in terms of b_2 and b_3 through the four integrals of (7). The relations are found to be

$$\begin{aligned}\frac{a_{20}}{Et^2} &= \frac{1}{16}\left[-\frac{\mu}{2}\left(\frac{b_2}{t}\right)^2 + 4\eta\alpha^2\right]\\ \frac{a_{02}}{Et^2} &= -\frac{1}{32\mu}\left(\frac{b_2}{t}\right)^2\\ \frac{a_{11}}{Et^2} &= \frac{\alpha}{(1+\mu)^2}(1-4\mu\eta)\frac{b_2}{t}\\ \frac{a_{22}}{Et^2} &= -\frac{\mu\eta^2\alpha^2}{(1+\mu)^2}\end{aligned} \quad (9)$$

In the above expressions, the dimensionless parameters are defined so that

$$\mu = \frac{n^2}{m^2} \quad (10)$$

$$\alpha = \frac{1}{m^2}\cdot\frac{R}{t} \quad (11)$$

$$\eta = \frac{b_3}{t\alpha} \quad (12)$$

The ratio n/m evidently represents the wave-length ratio in axial/circumferential directions.

The integration of (8) together with the relations given in (9) leads to the following two equations:

$$\alpha\phi = \frac{(1+\mu)^2}{12(1-\nu^2)} + \left\{\frac{1}{(1+\mu)^2} - \left[\frac{8}{(1+\mu)^2}+\frac{1}{2}\right]\mu\eta + \frac{16}{(1+\mu)^2}\mu^2\eta^2\right\}\alpha^2 + \frac{1+\mu^2}{16}\left(\frac{b_2}{t}\right)^2 \quad (13)$$

$$\alpha\phi = \frac{1+\mu^2}{3(1-\nu^2)} + \left[\frac{1}{4}+\frac{4\mu^2}{(1+\mu)^2}\eta^2\right]\alpha^2 + \left\{\frac{2\mu^2}{(1+\mu)^2} - \left[\frac{1}{2}\frac{1}{(1+\mu)^2}+\frac{1}{32}\right]\frac{\mu}{\eta}\right\}\left(\frac{b_2}{t}\right)^2 \quad (14)$$

The function ϕ on the left-hand sides of the above equations is a nondimensional stress parameter defined by the relation

$$\phi = \frac{\sigma R}{Et} - \mu\frac{pR^2}{Et^2} \quad (15)$$

For brevity, (13) and (14) may be rewritten as:

$$\alpha\phi = A_1 + (A_2 + A_3\eta + A_4\eta^2)\alpha^2 + A_5\left(\frac{b_2}{t}\right)^2 \quad (13a)$$

$$\alpha\phi = B_1 + (B_2 + B_4\eta^2)\alpha^2 + \left(B_5 + \frac{B_6}{\eta}\right)\left(\frac{b_2}{t}\right)^2 \quad (14a)$$

where

$$\begin{aligned}A_1 &= \frac{(1+\mu)^2}{12(1-\nu^2)}\\ A_2 &= \frac{1}{(1+\mu)^2}\\ A_3 &= -\left[\frac{8}{(1+\mu)^2}+\frac{1}{2}\right]\mu\\ A_4 &= \frac{16\mu^2}{(1+\mu)^2}\\ A_5 &= \frac{1+\mu^2}{16}\\ B_1 &= \frac{1+\mu^2}{3(1-\nu^2)}\\ B_2 &= \frac{1}{4}\\ B_4 &= \frac{4\mu^2}{(1+\mu)^2}\\ B_5 &= \frac{2\mu^2}{(1+\mu)^2}\\ B_6 &= -\left[\frac{1}{2(1+\mu)^2}+\frac{1}{32}\right]\mu\end{aligned} \quad (16)$$

The parameter (b_2/t) is eliminated between (13a) and (14a) and the stress parameter ϕ is expressed as

$$\phi = \frac{C_1 A_1}{\alpha} + C_2 A_2 \alpha \quad (17)$$

In the above equation,

$$C_1 = \frac{\frac{A_5}{A_1}B_1 - B_5 - \frac{B_6}{\eta}}{A_5 - B_5 - \frac{B_6}{\eta}} \quad (18)$$

$$C_2 = \frac{\left(\frac{A_5}{A_2}B_2 - \frac{A_3}{A_2}B_6 - B_5\right) - \frac{B_6}{\eta} - \left(\frac{A_3}{A_2}B_5 + \frac{A_4}{A_2}B_6\right)\eta + \left(\frac{A_5}{A_2}B_4 - \frac{A_4}{A_2}B_5\right)\eta^2}{A_5 - B_5 - \frac{B_6}{\eta}} \tag{19}$$

As can be seen from (15) to (19) the dimensionless variable $\sigma R/Et$ is a function of α, η, and μ. The buckling stress is thus obtained through minimization with respect to the parameters α, η, and μ. Differentiation of ϕ with respect to α is carried out first to obtain

$$\frac{\partial \phi}{\partial \alpha} = \frac{\partial \sigma}{\partial \alpha} = 0 \tag{20}$$

for p = constant. Thus from (17):

$$\alpha = \sqrt{\frac{C_1 A_1}{C_2 A_2}} \tag{21}$$

and finally from (17) with α given by (21)

$$\phi_\alpha = 2\sqrt{A_1 A_2}\ \sqrt{C_1 C_2} \tag{22}$$

The notation ϕ_α thus denotes the value of ϕ minimized with respect to α. The expressions for C_1 and C_2 are found from (18), (19), and (16). From (16):

$$\phi_\alpha = \sqrt{C_1 C_2}\ \sqrt{\frac{1}{3(1-\nu^2)}} \tag{22a}$$

It should be noted that $\sqrt{1/3(1-\nu^2)}$ is the classical coefficient from small-deflection theory for an unpressurized shell. When $\nu = 0.3$, $\sqrt{1/3(1-\nu^2)} = 0.606$. The minimization of ϕ with respect to η and μ is most easily obtained by numerical, or, rather, by graphic means. This is done by plotting ϕ_α in (22a) against η for each given value of μ. The minimum ϕ_α found from each of these curves is called $\phi_{\alpha,\eta}$, which should be equivalent to the value found from the relation $\partial\phi_\alpha/\partial\eta = 0$. Table 1 gives some of the numerical relations obtained in the course of this procedure.

TABLE 1

μ = 0	0.2	0.25	0.5	1.0	1.15
η =	0.59	0.53	0.325	0.18	0.11
$\phi_{\alpha,\eta}$ = 0.605	0.44	0.406	0.29	0.19	0.161

Let us introduce the following dimensionless parameters

$$\bar{\sigma} = \frac{\sigma R}{Et} \tag{23}$$

and

$$\bar{p} = \frac{pR^2}{Et^2} \tag{24}$$

Then (15) may be rewritten as

$$\bar{\sigma}_{\alpha,\eta} = \phi_{\alpha,\eta} + \mu\bar{p} \tag{25}$$

where $\bar{\sigma}_{\alpha,\eta}$ represents the minimized value of $\bar{\sigma}$ with respect to α and η. To find the dimensionless critical stress $\bar{\sigma}_{cr}$ at a given value of dimensionless pressure $\bar{p}$, several different values of μ are tried in (25) together with corresponding values of $\phi_{\alpha,\eta}$ from Table 1 until the right-hand side of (25) is minimized. The value of μ, at which $\bar{\sigma}_{\alpha,\eta}$ is minimum and equals $\bar{\sigma}_{cr}$, is called μ_{cr}. Some values of $\bar{\sigma}_{cr}$ and μ_{cr} for various values of $\bar{p}$ are given in Table 2.

TABLE 2

$\bar{p}$ = 0	0.01	0.05	0.1	0.2	0.4	0.6	0.8
μ_{cr} = 1.15	1.10	1.08	1.04	0.76	0.45	0.24	0.08
$\bar{\sigma}_{cr}$ = 0.161	0.176	0.227	0.283	0.37	0.481	0.56	0.6

It can be seen that μ_{cr} decreases with increasing $\bar{p}$. This indicates that the buckling wave becomes longer in the circumferential direction when the pressure increases.

The relation between $\bar{\sigma}_{cr}$ and $\bar{p}$ is shown in Fig. 1 as Curve II. The results from [4] and [5] and the test data from [6] and [7] are plotted in this figure also. The broken curve shown there represents the curve best fitting the data in [5], [6], and [7]. The predictions of the present theory are shown as Curve II in Fig. 2 so as to afford a comparison with experimental data given in [9].

In Fig. 1, the broken curve indicates that $\bar{\sigma}_{cr}$ is only about 0.09 at $\bar{p} = 0$, and $\bar{\sigma}_{cr}$ increases from 0.09 to approximately 0.35, then levels off at higher values of $\bar{p}$. However, $\bar{\sigma}_{cr}$ is expected to reach the classical value of 0.606 when the value of $\bar{p}$ is relatively high. One of the most probable causes of the lower result indicated by the broken curve corresponding to test data lies in initial imperfections which in general increase with increasing R/t. If the imperfection factor does not vary significantly due to the change of $\bar{p}$, then the ratio of $\bar{\sigma}_{cr}$ at two different pressures will be nearly independent of the effect of imperfections. Let $\bar{\sigma}_{cr,o}$ represent $\bar{\sigma}_{cr}$ at $\bar{p} = 0$, and

$$\Delta\bar{\sigma}_{cr} = \bar{\sigma}_{cr} - \bar{\sigma}_{cr,o}$$

The ratio, $\Delta\bar{\sigma}_{cr}/\bar{\sigma}_{cr,o}$, is plotted against $\bar{p}$ in Fig. 3. As shown in this figure, the predictions of the present theory are in reasonably good agreement with experimental evidence, which is re-plotted from the broken curve of Fig. 1. One advantage of introducing the ratio $\Delta\bar{\sigma}_{cr}/\bar{\sigma}_{cr,o}$ is that the relation in Fig. 3 can be used having test data at only one pressure to predict the critical stress in the same imperfect shell at any other pressure. For instance, a test is made at $\bar{p} = 0.4$, for

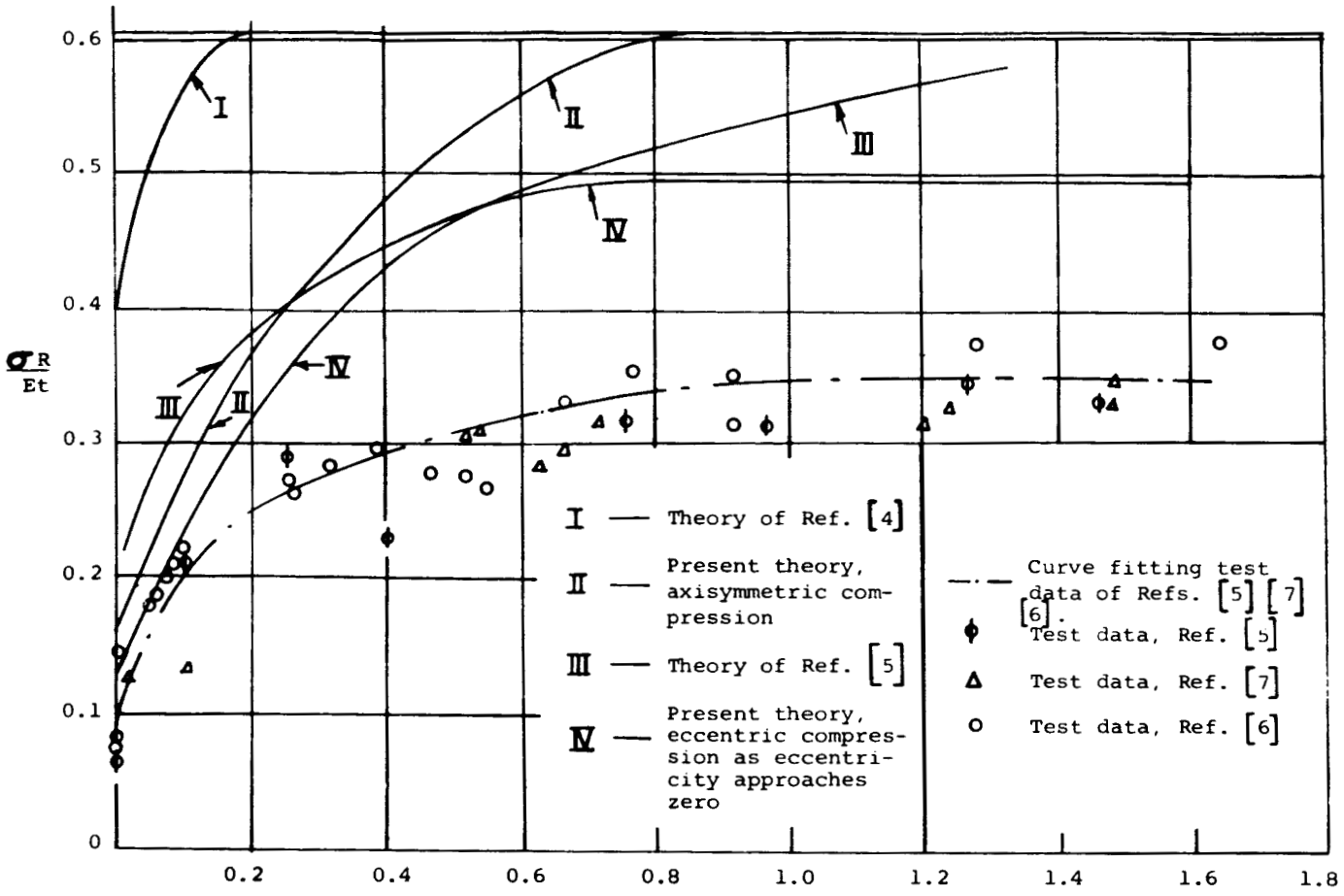

FIGURE 1. POSTBUCKLING BEHAVIOR OF AXIALLY COMPRESSED PRESSURIZED CYLINDRICAL SHELLS.

which value $\bar{\sigma}_{cr}$ is found experimentally to be 0.29. From Fig. 3, the present analysis gives $\Delta\bar{\sigma}_{cr}/\bar{\sigma}_{cr,o} = 2.02$. Therefore, it can be predicted that $\bar{\sigma}_{cr} = 0.096$, 0.221, and 0.356 at $\bar{p} = 0$, 0.2, and 0.8, respectively, while the mean test data from Fig. 1 shows that $\bar{\sigma}_{cr} = 0.09$, 0.25, and 0.34 at $\bar{p} = 0$, 0.2, and 0.8, respectively.

Eccentric Compression, Pure Bending

When a cylindrical shell is subject either to pure bending or eccentrically applied compression k in (3) and (8) is unity. The solution in this case is analogous to the solution of the previous section. The coefficients of the Airy stress function F are found to be

$$\frac{a_{20}}{Et^2} = \frac{1}{16}\left[2\eta\alpha^2 - \left(\frac{3}{16}\mu - \frac{1}{16m^2}\right)\left(\frac{b_2}{t}\right)^2\right]$$

$$\frac{a_{02}}{Et^2} = -\frac{3}{256\mu}\left(\frac{b_2}{t}\right)^2$$

$$\frac{a_{11}}{Et^2} = \frac{\alpha\left[1 - \left(3\mu + \frac{1}{4m^2}\right)\eta\right]\left(\frac{b_2}{t}\right)}{2(1+\mu)^2} \qquad (26)$$

$$\frac{a_{22}}{Et^2} = -\frac{\left(6\mu + \frac{1}{2m^2}\right)\eta^2\alpha^2 + \frac{1}{16m^2}\left(\frac{b_2}{t}\right)^2}{16(1+\mu)^2}$$

where μ, α, and η are given by (10), (11), and (12), respectively.

From (8) and (26),

$$\alpha\phi_1 = \frac{1}{(1-\nu^2)}\left[\frac{(1+\mu)^2}{8} + \frac{1}{12m^2}\left(1+3\mu+\frac{1}{2m^2}\right)\right] + \left\{\frac{1}{(1+\mu)^2}\right.$$
$$\left. - \left[\frac{6\mu+\frac{1}{2m^2}}{(1+\mu)^2} + \frac{3\mu+\frac{1}{m^2}}{8}\right]\eta + \left[\frac{576\mu^2+108\frac{\mu}{m^2}+\frac{5}{m^4}}{64(1+\mu)^2}\right]\eta^2\right\}\alpha^2$$
$$+ \left[\frac{9+9\mu^2+\frac{6\mu}{m^2}+\frac{1}{m^4}}{256} + \frac{1}{m^4}\cdot\frac{1}{512(1+\mu)^2}\right]\left(\frac{b_2}{t}\right)^2 \qquad (27)$$

$$\alpha\phi_2 = \frac{1}{2(1-\nu^2)}\left[(1+\mu^2) + \frac{1}{6m^2}\left(1+3\mu+\frac{1}{4m^2}\right)\right]$$
$$+ \left[\frac{1}{4} + \left\{\frac{144\mu^2+\frac{24\mu}{m^2}+\frac{1}{m^4}}{64(1+\mu)^2}\right\}\eta^2\right]\alpha^2 \qquad (28)$$
$$+ \left\{\frac{576\mu^2+108\frac{\mu}{m^2}+\frac{5}{m^4}}{512(1+\mu)^2} - \left[\frac{12\mu+\frac{1}{m^2}}{32(1+\mu)^2} + \frac{3\mu+\frac{1}{m^2}}{128}\right]\frac{1}{\eta}\right\}\left(\frac{b_2}{t}\right)^2$$

The stress parameters ϕ_1 and ϕ_2 are defined by the relations

$$\phi_1 = \frac{\sigma_b R}{Et} + \frac{3}{2}\cdot\frac{\sigma_c R}{Et} - \frac{1}{2}\left(3\mu + \frac{1}{m^2}\right)\frac{pR^2}{Et^2}$$
$$\phi_2 = \frac{\sigma_b R}{Et} + \frac{3}{2}\cdot\frac{\sigma_c R}{Et} - \frac{1}{2}\left(3\mu + \frac{1}{2m^2}\right)\frac{pR^2}{Et^2} \qquad (29)$$

The experiments of Suer, Harris, Skene, and Benjamin [9] indicate that shells subject to compression or bending will buckle into a multiple wave pattern in the logitudinal direction. Numerical results from the present analysis also indicate that m has a magnitude greater than 10 when R/t is greater than 500. These calculations are too lengthy to present, but for example: At $\bar{p} = 0.48$ and $R/t = 1{,}000$, it was found that $1/m^2 = 0.00204$, which is much less than unity. The value of α is usually in the neighborhood of unity; hence, from (11) m^2 varies approximately as R/t. In the present analysis we are concerned only with extremely thin shells; hence this ratio is large. Therefore, for practical purposes $1/m^2$ and $1/m^4$ are negligible compared to unity. Thus,

$$\phi_1 = \phi_2 = \phi_b = \frac{\sigma_b R}{Et} + \frac{3}{2}\frac{\sigma_c R}{Et} - \frac{3}{2}\mu\frac{pR^2}{Et^2} \qquad (30)$$

$$\alpha\phi_b = \frac{1}{(1-\nu^2)}\cdot\frac{(1+\nu)^2}{8}\left\{\frac{1}{(1+\mu)^2} - \mu\left[\frac{6}{(1+\mu)^2} + \frac{3}{8}\right]\eta + \frac{9\mu^2}{(1+\mu)^2}\eta^2\right\}\alpha^2 + \frac{9(1+\mu)^2}{256}\left(\frac{b_2}{t}\right)^2 \qquad (31)$$

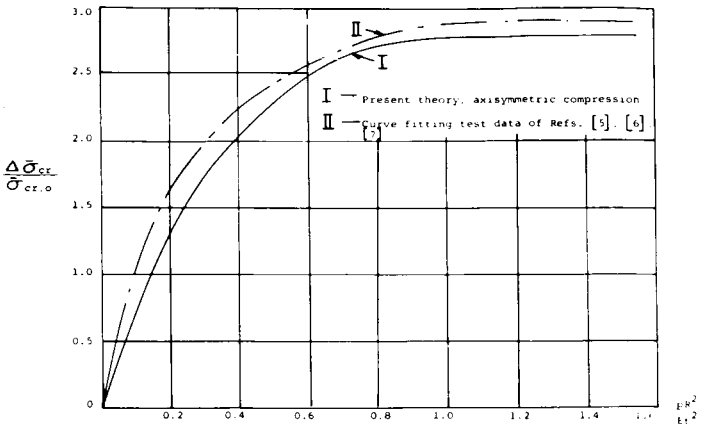

FIGURE 3. PREDICTIONS OF PRESENT THEORY AND TEST DATA FOR AXIALLY COMPRESSED PRESSURIZED CYLINDRICAL SHELLS

and

$$\alpha\phi_b = \frac{1+\mu^2}{2(1-\nu^2)} + \left[\frac{1}{4} + \frac{9\mu^2}{4(1+\mu)^2}\eta^2\right]\alpha^2 + \left\{\frac{9}{8}\cdot\frac{\mu^2}{(1+\mu)^2} - \left[\frac{1}{8(1+\mu)^2} + \frac{1}{128}\right]\frac{3\mu}{\eta}\right\}\left(\frac{b_2}{t}\right)^2 \qquad (32)$$

For brevity, (31) and (32) may be rewritten as:

$$\alpha\phi_b = \bar{A}_1 + (\bar{A}_2 + \bar{A}_3\eta + \bar{A}_4\eta^2)\alpha^2 + \bar{A}_5\left(\frac{b_2}{t}\right)^2 \qquad (31a)$$

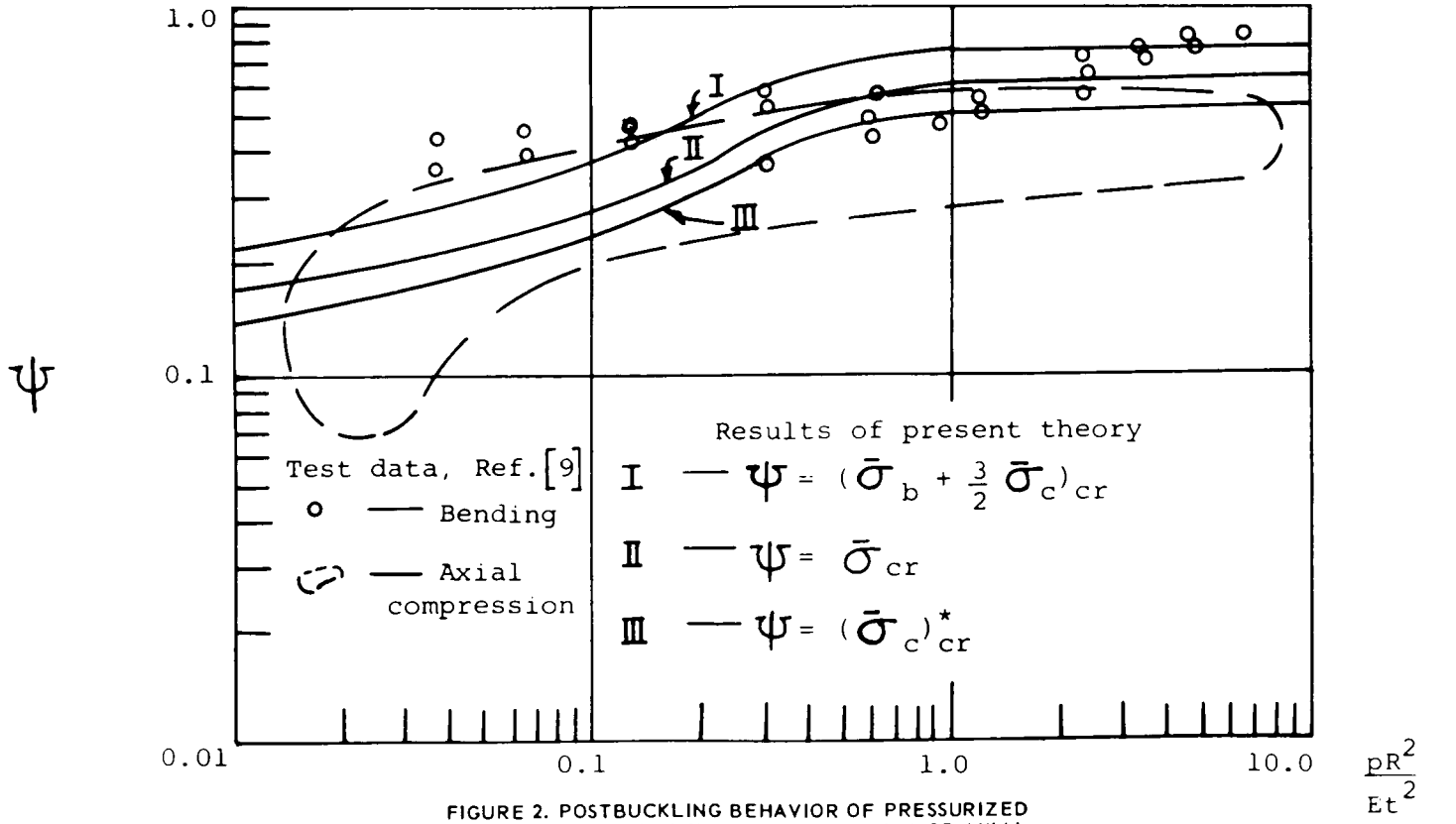

FIGURE 2. POSTBUCKLING BEHAVIOR OF PRESSURIZED CYLINDRICAL SHELLS SUBJECT TO BENDING OR AXIAL COMPRESSION.

and

$$\alpha\phi_b = \bar{B}_1 + (\bar{B}_2 + \bar{B}_4\eta^2)\alpha^2 + \left(\bar{B}_5 + \frac{\bar{B}_6}{\eta}\right)\left(\frac{b_2}{t}\right)^2 \tag{32a}$$

where

$$\bar{A}_1 = \frac{(1+\mu)^2}{8(1-\nu^2)}$$

$$\bar{A}_2 = \frac{1}{(1+\mu)^2}$$

$$\bar{A}_3 = -\left[\frac{6}{(1+\mu)^2} + \frac{3}{8}\right]\mu$$

$$\bar{A}_4 = \frac{9\mu^2}{(1+\mu)^2}$$

$$\bar{A}_5 = \frac{9(1+\mu^2)}{256} \tag{33}$$

$$\bar{B}_1 = \frac{1+\mu^2}{2(1-\nu^2)}$$

$$\bar{B}_2 = \frac{1}{4}$$

$$\bar{B}_4 = \frac{9\mu^2}{4(1+\mu)^2}$$

$$\bar{B}_5 = \frac{9\mu^2}{8(1+\mu)^2}$$

$$\bar{B}_6 = -\left[\frac{3}{8(1+\mu)^2} + \frac{3}{128}\right]\mu$$

Further,

$$\bar{C}_1 = \frac{\dfrac{\bar{A}_5}{\bar{A}_1}\bar{B}_1 - \bar{B}_5 - \dfrac{\bar{B}_6}{\eta}}{\bar{A}_5 - \bar{B}_5 - \dfrac{\bar{B}_6}{\eta}}$$

$$\bar{C}_2 = \frac{\dfrac{\bar{A}_5}{\bar{A}_2}\bar{B}_2 - \bar{B}_5 - \dfrac{\bar{A}_3}{\bar{A}_2}\bar{B}_6 - \dfrac{\bar{B}_6}{\eta} - \left(\dfrac{\bar{A}_3}{\bar{A}_2}\bar{B}_5 + \dfrac{\bar{A}_4}{\bar{A}_2}\bar{B}_6\right)\eta + \left(\dfrac{\bar{A}_5}{\bar{A}_2}\bar{B}_4 - \dfrac{\bar{A}_4}{\bar{A}_2}\bar{B}_5\right)\eta^2}{\bar{A}_5 - \bar{B}_5 - \dfrac{\bar{B}_6}{\eta}} \tag{34}$$

The simultaneous solution of (31a) and (32a) leads to

$$\phi_b = \frac{\bar{C}_1\bar{A}_1}{\alpha} + \bar{C}_2\bar{A}_2\alpha \tag{35}$$

From the relation $\partial\phi_b/\partial\alpha = 0$ and (35),

$$\alpha = \sqrt{\frac{\bar{C}_1\bar{A}_1}{\bar{C}_2\bar{A}_2}} \tag{36}$$

and finally from (35) with α given by (36)

$$(\phi_b)_\alpha = 2\sqrt{\bar{A}_1\bar{A}_2}\sqrt{\bar{C}_1\bar{C}_2} = \sqrt{\bar{C}_1\bar{C}_2}\,\sqrt{\frac{1}{2(1-\nu^2)}} \tag{37}$$

where $(\phi_b)_\alpha$ is the value of ϕ_b minimized with respect to α. For classical small deflection theory, $\eta = 0$; hence, $C_1 = C_2 = 1$ and the expression $\sqrt{1/2(1-\nu^2)}$ is the coefficient for this theory. When $\nu = 0.3$, $\sqrt{1/2(1-\nu^2)} = 0.74$.

Analogous to the solution in the case of axisymmetric compression, the minimization of ϕ_b with respect to μ and η is done graphically. First, $(\phi_b)_\alpha$ versus η is plotted for various values of μ. The minimum $(\phi_b)_\alpha$ found from each of these curves is called $(\phi_b)_{\alpha,\eta}$. Table 3 gives some of the numerical relations obtained in the course of this procedure.

TABLE 3

μ	$= 0$	0.25	0.5	1.0	1.15
η	$=$	0.66	0.46	0.23	0.15
$(\phi_b)_{\alpha,\eta}$	$= 0.74$	0.52	0.34	0.21	0.195

Let us introduce the following dimensionless parameters

$$\bar{\sigma}_b = \frac{\sigma_b R}{E t}$$

and (38)

$$\bar{\sigma}_c = \frac{\sigma_c R}{E t}$$

Thus, from (30)

$$\left(\bar{\sigma}_b + \frac{3}{2}\bar{\sigma}_c\right)_{\alpha,\eta} = (\phi_b)_{\alpha,\eta} + \frac{3}{2}\mu\bar{p} \tag{39}$$

To find the dimensionless critical stress $\left(\bar{\sigma}_b + \frac{3}{2}\bar{\sigma}_c\right)_{cr}$ at a given value of dimensionless pressure $\bar{p}$, several different values of μ are tried in (39), together with corresponding values of $(\phi_b)_{\alpha,\eta}$ from Table 3 until the right-hand side of (39) is minimized.

The value of μ at which $\left(\bar{\sigma}_b + \frac{3}{2}\bar{\sigma}_c\right)_{\alpha,\eta}$ is minimum and equals $\left(\bar{\sigma}_b + \frac{3}{2}\bar{\sigma}_c\right)_{cr}$ is called μ_{cr}. Table 4 indicates some numerical relations in terms of the pressure.

TABLE 4

$\bar{p}$	$= 0$	0.025	0.05	0.1	0.2	0.4	0.6	0.8
μ_{cr}	$= 1.14$	1.1	1.04	0.86	0.63	0.34	0.14	0.02
$(\bar{\sigma}_b + \frac{3}{2}\bar{\sigma}_c)_{cr}$	$= 0.2$	0.249	0.294	0.365	0.48	0.64	0.73	0.734
$(\bar{\sigma}_c)^*_{cr}$	$= 0.133$	0.166	0.196	0.243	0.32	0.426	0.487	0.489

It can be seen that μ_{cr} decreases with increasing $\bar{p}$. In the above table, $(\bar{\sigma}_c)^*_{cr}$ stands for the value of $(\bar{\sigma}_c)_{cr}$ when $\bar{\sigma}_b \to 0$. The relations between $\left(\bar{\sigma}_b + \frac{3}{2}\bar{\sigma}_c\right)_{cr}$ and $\bar{p}$ as

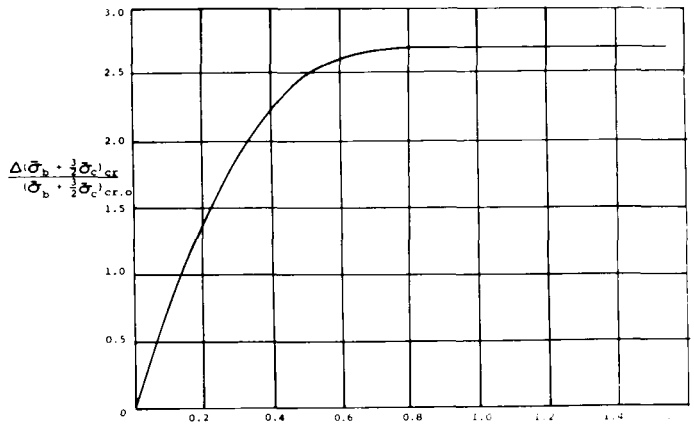

FIGURE 4. INCREMENT OF CRITICAL STRESS AS A FUNCTION OF PRESSURE FOR CYLINDRICAL SHELLS SUBJECT TO ECCENTRIC COMPRESSION OR PURE BENDING.

well as $(\bar{\sigma}_c)^*_{cr}$ and $\bar{p}$ are shown in Fig. 2, in which the data from [9] is shown also.

The broken curve shown there bounds test data obtained by Suer, Harris, Skene, and Benjamin [9] for axial compression. Bending test data due to these same authors is shown by individual points in Fig. 2.

Let us introduce the notation

$$\Delta\left(\bar{\sigma}_b + \frac{3}{2}\bar{\sigma}_c\right)_{cr} = \left(\bar{\sigma}_b + \frac{3}{2}\bar{\sigma}_c\right)_{cr} - \left(\bar{\sigma}_b + \frac{3}{2}\bar{\sigma}_c\right)_{cr,o} \quad (40)$$

where $\left(\bar{\sigma}_b + \frac{3}{2}\bar{\sigma}_c\right)_{cr,o}$ represents the value of $\left(\bar{\sigma}_b + \frac{3}{2}\bar{\sigma}_c\right)_{cr}$ at $\bar{p} = 0$. The ratio $\dfrac{\Delta\left(\bar{\sigma}_b + \frac{3}{2}\bar{\sigma}_c\right)_{cr}}{\left(\bar{\sigma}_b + \frac{3}{2}\bar{\sigma}_c\right)_{cr,o}}$ is plotted against $\bar{p}$. in Fig. 4. Again, this ratio should predict the critical stress in an imperfect shell from test data at only one pressure.

It has been observed that generally $(\bar{\sigma}_c)^*_{cr}$ is not equal to the value of $\bar{\sigma}_{cr}$ found for axisymmetric compression. The difference is due to the deflection patterns employed. Curves II and III of Fig. 2 indicate the effect on axial compression of those different patterns and show that even a slight eccentricity in application of load will greatly reduce the buckling stress. $(\bar{\sigma}_c)^*_{cr}$ versus $\bar{p}$ is shown in Fig. 1 as Curve IV.

Discussion and Conclusions

It can be observed that $\mu = 0$ in the case of ring buckling and further, $b_3 = \eta = 0$ in the case of small deflections. If either μ or b_3 is zero, the above analysis reduces to a small deflection solution.

The ratio between stresses, $\left(\bar{\sigma}_b + \frac{3}{2}\bar{\sigma}_c\right)_{cr} \Big/ \bar{\sigma}_{cr}$, is approximately 1.25 and varies only slightly with pressure. Therefore, the ratio $\dfrac{(\bar{\sigma}_c)^*_{cr}}{\bar{\sigma}_{cr}}$ is 0.833. The procedure indicated can be employed when test data at one pressure are available to predict the critical stress in the same imperfect shell at any other pressure. Since more consistent test results can be expected from shells under higher pressures. Figs. 3 and 4 are available to predict the buckling stresses when at least one test has been made on some moderately pressurized cylinders. For instance, if the critical pure bending stress, $(\sigma_b R/Et)_{cr}$, has been found experimentally as 0.53 at $\bar{p} = 0.4$, then from Fig. 4 one can find $(\sigma_b R/Et)_{cr} = 0.163$, and 0.603 at $\bar{p} = 0$, and 0.8, respectively. This evaluation is applied only to shells having the same ratio R/t. The effects due to a change of R/t will be discussed in a later paper.

The predictions of the present theory for pressurized axially compressed cylindrical shells are in substantial agreement with test data for a rather wide range of values of internal pressure. Predictions of the theory for pressurized cylindrical shells in pure bending are in reasonable agreement with experimental evidence for dimensionless internal pressures in excess of 0.1 but are conservative for smaller values of internal pressure.

References

1. Donnell, L. H., "A New Theory for the Buckling of Thin Cylinders Under Axial Compression and Bending," *Transactions of the ASME*, Vol. 56, No. 11, pp. 795-806, November, 1934.

2. von Kármán, T., and Tsien, H. S., "The Buckling of Thin Cylindrical Shells Under Axial Compression," *Journal of the Aeronautical Sciences*, Vol. 8, No. 8, pp. 303-312, June, 1941.

3. Kempner, J., "Postbuckling Behavior of Axially Compressed Cylindrical Shells," *Journal of the Aeronautical Sciences*, Vol. 21, No. 5, pp. 329-335, May, 1954.

4. Lo, H., Crate, H., and Schwartz, E. B., "Buckling of Thin-Walled Cylinder Under Axial Compression and Internal Pressure," *NACA TN 2021*, January, 1950.

5. Thielemann, W. F., "New Development in the Nonlinear Theories of the Buckling of Thin Cylindrical Shells," in *Aeronautics and Astronautics*, Pergamon Press, pp. 76-121, New York, 1960.

6. Fung, Y. C., and Sechler, E. E., "Buckling of Thin-Walled Circular Cylinders Under Axial Compression and Internal Pressure," *Journal of the Aeronautical Sciences*, Vol. 24, No. 5, pp. 351-356, May, 1957.

7. Lofblad, R. P., Jr., "Elastic Stability of Thin-Walled Cylinders and Cones with Internal Pressure Under Axial Compression," *MIT Technical Report 25-29*, May 1959.

8. Seide, P., and Weingarten, V. I., "On the Buckling of Circular Cylindrical Shells Under Pure Bending," *Journal of Applied Mechanics*, Vol. 28, No. 1, pp. 112-116, March, 1961.

9. Suer, H. S., Harris, L. A., Skene, W. T., and Benjamin, R. J., "The Bending Stability of Thin-Walled Unstiffened Circular Cylinders Including the Effect of Internal Pressure," *Journal of the Aeronautical Sciences*, Vol. 25, No. 5, pp. 281-287, May, 1958.

PUBLICATIONS OF THE FLORIDA

ENGINEERING AND INDUSTRIAL EXPERIMENT STATION

The Engineering and Industrial Experiment Station, College of Engineering, issues five series of publications under the general title, *ENGINEERING PROGRESS at the University of Florida:* (1) Bulletin Series – original publications of research, or conference proceedings, usually on problems of specific interest to the industries of the State of Florida; (2) Technical Paper Series – reprints of technical articles by staff members appearing in national publications; (3) Leaflet Series – nontechnical articles of a general nature written by staff members; (4) Technical Progress Reports – reports of research which is still in progress, and (5) Florida Engineering Series – books on technical engineering problems.

A complete list of these publications is available upon request to:

The Editor
Florida Engineering and Industrial Experiment Station
University of Florida
Gainesville, Florida